Finite-temperature real-energy-axis solutions of the isotropic Eliashberg integral equations

M. J. Holcomb

Departments of Chemistry and Physics, Stanford University, Stanford, California 94305
(Received 15 June 1995; revised manuscript received 7 February 1996)

A fast, efficient algorithm has been developed for calculating the finite-temperature real-energy-axis solutions of the Eliashberg integral equations for an arbitrary form of the electron-boson coupling function and Coulomb repulsion. Using this algorithm, the complex superconducting gap function $\Delta(\omega,T)$, and the complex renormalization function $Z(\omega,T)$, have been obtained for a variety of forms of the electron-boson coupling spectrum. In addition, by calculating $\Delta(\omega,T)$ at finite temperatures, the superconducting critical temperature T_c has been obtained for a variety of model systems. These results compare well with the approximate analytic expression derived by Allen and Dynes for values of λ less than 0.75. The solution of the Eliashberg equations has also been obtained for a model in which there are two well separated peaks in the electron-phonon coupling spectrum. This form of coupling spectrum is found to be particularly effective in raising the T_c of the model system. Further, this model has been extended and the solution of the Eliashberg equations has been obtained with an electron-boson coupling spectrum consisting of both an electron-phonon component and a high-energy electronic electron-boson component. This form of the electron-boson coupling function may have special significance in the field of high-temperature superconductivity. [S0163-1829(96)09234-X]

I. INTRODUCTION

The most detailed microscopic theory of superconductivity, which accounts for virtually all experimentally observed phenomena in conventional phonon-mediated superconductors, was derived by Eliashberg in 1960.[1] The Eliashberg equations are a generalization of the microscopic theory of superconductivity derived three years earlier by Bardeen, Cooper, and Schrieffer (BCS),[2] but which include the retarded effects of the electron-phonon interaction. In contrast to BCS theory, the Eliashberg equations describe the superconducting gap as a complex, energy-dependent function whose structure reflects the energy dependence of the underlying electron-phonon interaction. Given the electron-phonon coupling spectrum, the magnitude of the screened electron-electron repulsion, and the electronic density of states in the normal state, the results of the theory are remarkably accurate.[3] Eliashberg theory accounts for most experimentally observed phenomena in phonon-mediated superconductors, including the many significant deviations from weak-coupling BCS behavior.[4,5] Among the most common experimentally determined quantities are measurements of the superconducting critical temperature T_c, the superconducting density of states, the temperature dependence of the superconducting gap, the temperature dependence of the London penetration depth, the temperature dependence of the electronic specific heat, and the temperature dependence of the electronic spin-lattice relaxation rate.[6–8] In principle, these measurements yield information about the underlying electron-pairing mechanism which results in the superconductivity. By providing a reliable, well-tested link between experiment and theory, the Eliashberg integral equations are an indispensable tool to experimentalists in the field of superconductivity.

Although Eliashberg theory is remarkably complete in its description of the superconducting state given accurate input parameters, it remains relatively inaccessible as a common interpretive tool for experimentalists in the field of superconductivity largely because of the inherent complexity of the equations themselves. The Eliashberg equations form a coupled set of nonlinear integral equations which determine both the complex superconducting gap function $\Delta(\omega,T)$, and the complex renormalization function $Z(\omega,T)$. In this formalism, $\Delta(\omega,T)$ reflects the strength of the electron-electron pairing potential and $Z(\omega,T)$ reflects the enhancement of the electron mass which results from the electron-phonon interaction in phonon-mediated superconductors.

While these equations have been used over the past 30 years for the treatment of tunneling data, optical spectra, and many other experiments, these have generally been done only after certain approximations have been made. Recently, the need arose for a much more precise solution to these equations[9,10] such that they could describe the relative changes in the density of electronic states in the superconducting state accurate to approximately one part in 10^5. Earlier methods were found to be inadequate. The algorithms described here were developed to correct this inadequacy and lead to solutions which are internally consistent to this accuracy. These solutions cast new light on the physics of both high- and low-temperature superconductors and are discussed in Sec. IV D.

Historically, two distinct methods have been developed for solving the Eliashberg equations; a direct method which involves evaluating the required integrals on the real-energy axis until a self-consistent solution is obtained, and an indirect method in which the problem is solved self-consistently on the imaginary-energy axis. The latter approach is commonly referred to as the Matsubara method.[3,11–14] The Matsubara method at low temperatures has the advantage of being computationally more efficient because the superconducting gap function at imaginary energies $\Delta(i\omega)$, can be obtained easily by summing over only a small number of discrete poles located on the imaginary-energy axis.[13] It has the disadvantage, however, of being an inherently less

intuitive method of solving the equations. Furthermore, in order to compare the results of the theory with experiment, it is necessary to obtain the superconducting gap function on the real-energy axis. For example, $\Delta(\omega)$ is required in the interpretation of the conductance versus bias voltage spectrum of a normal/insulator/superconductor ($N/I/S$) tunneling junction.[5,15] Measurements such as these have provided the most convincing experimental proof that the superconductivity in low-temperature superconductors is mediated strictly via the electron-phonon interaction. Since the deviations in the tunneling conductance which result from the presence of $\Delta(\omega)$ are typically less than 1%, it is of great importance that the calculated real-energy-axis gap function be of sufficient accuracy. The earliest analytic continuation of the Matsubara gap function to the real-energy axis reproduced the magnitude of $\Delta(\omega,T)$ only at low energies and temperatures.[16] Because this method could not reproduce the structure in $\Delta(\omega,T)$ at the phonon energies, it could not be used in an inversion procedure to obtain the electron-phonon coupling spectrum. Recently, a method has been developed which can, in principle, accurately reproduce $\Delta(\omega)$ from the Matsubara gap function.[17] Using this procedure, $\Delta(\omega)$ can be obtained with no iterations in the limit of zero temperature. At finite temperatures, however, this method requires several iterations to converge. In any case, obtaining the solution of the Eliashberg equations using the Matsubara method, and analytically continuing $\Delta(i\omega)$ to the real-energy axis, has been limited to relatively low temperatures. At intermediate temperatures, the sum over the imaginary-energy poles may not converge as rapidly and the cutoff limit of this sum may affect both the resulting magnitude, and functional form of the superconducting gap function on the real-energy axis.[14]

The earliest solutions of the Eliashberg equations were obtained by performing the required integrations on the real-energy axis.[15,18–20] Usually, these solutions were obtained in the extreme limits of zero temperature[15,18] or at a temperature very near T_c.[19,20] In each limit there exists significant simplifications which dramatically reduce the difficulty in computing the solution. Finding the solution of the real-energy-axis Eliashberg equations involves the calculation of many principal part integrals. This task, though not difficult, may be time consuming, and unfortunately does not lend itself to a straightforward computation. In the full finite-temperature form of the real-energy-axis Eliashberg equations it is necessary to calculate many thousands of principal part integrals, take into account the effects of finite temperature by including all Fermi and Bose thermal occupation factors, and properly account for all integrable singularities which may occur at energies near the superconducting gap edge.

In order to compare experimentally measured quantities with the predictions of Eliashberg theory, it is often necessary to calculate $\Delta(\omega)$ at finite temperatures. Because experiments are rarely carried out at zero temperature or at temperatures very close to T_c, the solution of the Eliashberg equations at intermediate temperatures is required. This is, in fact, less of a problem with weak-coupling phonon-mediated superconductors because $\Delta(\omega,T)$ can be approximated by multiplying the zero-temperature gap function by a scaling factor representing the known temperature dependence of the BCS gap.[19] This approximation, however, is invalid for strong-coupling superconductors where, in addition to a reduction of the superconducting gap at finite temperatures, there is also a significant change in the functional form of $\Delta(\omega,T)$. Alternatively, if the T_c of the material is high enough so the phonon populations are significant at these elevated temperatures, then the additional structure in $\Delta(\omega,T)$ at high temperatures must be included in the interpretation of experimental results. This may be of particular importance in the interpretation of experiments performed on the high-temperature cuprate superconductors. With critical temperatures on the order of 100 K, and significant electron-phonon coupling as evidenced through $N/I/S$ tunneling[21] and femtosecond pulse-probe measurements,[22,23] the interpretation of any experiment performed on the high-temperature superconductors must take into account the temperature at which the measurement was carried out and properly solve for the associated $\Delta(\omega,T)$. Because of the inherent problems associated with obtaining the Matsubara gap function at high temperatures, and analytically continuing this to the real-energy axis, obtaining $\Delta(\omega,T)$ at high temperatures is most easily accomplished using the real-energy-axis formulation of the Eliashberg equations.

We have developed a fast, computationally efficient algorithm for calculating the real-energy-axis, finite-temperature solutions to the Eliashberg equations with an arbitrary form of the electron-boson coupling function. We have used this algorithm to calculate $\Delta(\omega,T)$, $Z(\omega,T)$, and T_c of model systems based upon a variety of electron-boson coupling spectra. We find that the analytic T_c expression defined by McMillan[20] and later refined by Allen and Dynes[13] provides an approximate value for the T_c of these model systems. But, in order to obtain for these models a value of T_c with sufficient accuracy to use the theory as a framework to describe experimental data, we find that the Eliashberg equations must be solved at finite temperatures. This is because the value of T_c given by the expression of Allen and Dynes can differ from the actual T_c by as much as 15%.[14]

We also discuss the solutions of the Eliashberg equations based upon a model of the electron-boson coupling function in which there are two well-separated peaks in the coupling spectrum. We first present results obtained from a purely electron-phonon based interaction, and then extend the model to calculate the solution of the Eliashberg equations based upon a electron-boson coupling function which consists of *both* an electron-phonon interaction *and* an electronic electron-boson interaction. This model may have particular significance in the field of high-temperature superconductivity where the microscopic mechanism which is responsible for the high critical temperatures of the cuprate superconductors is not yet known.

II. FORMALISM

In this development, we assume the conventional approximations upon which Eliashberg theory is developed are appropriate.[1] The most important of these being the validity of Migdal's theorem[3] in each model electron-boson coupling function. We also assume that the model material is isotropic. In this case, the electron-boson coupling spectrum $G(\Omega)$, represents the strength of electron-boson coupling, at energy Ω, averaged over the Fermi surface.[15] In the case where the

superconductivity is solely mediated through the electron-phonon interaction, $G(\Omega)$ is more precisely written as $\alpha^2(\Omega)F(\Omega)$ where $\alpha^2(\Omega)$ is the square of the electron-phonon matrix element and $F(\Omega)$ is the phonon density of states. These assumptions result in the most popular form of the real-energy-axis Eliashberg equations, that is, the form in which the remaining integrations are strictly over energy variables. Using these model assumptions, the finite-temperature, real-energy-axis Eliashberg equations as derived by Scalapino[4] can be written as

$$\Delta(\omega,T) = \frac{1}{Z(\omega,T)} \int_0^\infty d\omega' \mathrm{Re}\left\{ \frac{\Delta(\omega',T)}{\sqrt{\omega'^2 - \Delta^2(\omega',T)}} \right\}$$

$$\times K_+(\omega,\omega',T) - \frac{\mu^*}{Z(\omega,T)} \int_0^\infty d\omega'$$

$$\times \mathrm{Re}\left\{ \frac{\Delta(\omega',T)}{\sqrt{\omega'^2 - \Delta^2(\omega',T)}} \right\} \tanh\left(\frac{\beta\omega'}{2} \right), \quad (1)$$

with

$$Z(\omega,T) = 1 - \frac{1}{\omega} \int_0^\infty d\omega' \mathrm{Re}\left\{ \frac{\omega'}{\sqrt{\omega'^2 - \Delta^2(\omega',T)}} \right\}$$

$$\times K_-(\omega,\omega',T), \quad (2)$$

$$K_+(\omega,\omega',T) = \int_0^\infty d\Omega\, G(\Omega)\left[\frac{f(-\omega') + n(\Omega)}{\omega' + \omega + \Omega} \right.$$

$$+ \frac{f(-\omega') + n(\Omega)}{\omega' - \omega + \Omega} - \frac{f(\omega') + n(\Omega)}{-\omega' + \omega + \Omega}$$

$$\left. - \frac{f(\omega') + n(\Omega)}{-\omega' - \omega + \Omega} \right], \quad (3)$$

$$K_-(\omega,\omega',T) = \int_0^\infty d\Omega\, G(\Omega)\left[\frac{f(-\omega') + n(\Omega)}{\omega' + \omega + \Omega} \right.$$

$$- \frac{f(-\omega') + n(\Omega)}{\omega' - \omega + \Omega} + \frac{f(\omega') + n(\Omega)}{-\omega' + \omega + \Omega}$$

$$\left. - \frac{f(\omega') + n(\Omega)}{-\omega' - \omega + \Omega} \right], \quad (4)$$

and

$$f(\omega) = \left(\frac{1}{\exp(\beta\omega) + 1} \right), \quad n(\omega) = \left(\frac{1}{\exp(\beta\omega) - 1} \right),$$

where $\Delta(\omega,T)$ is the complex, energy-, and temperature-dependent superconducting gap function, $Z(\omega,T)$ is the complex, energy-, and temperature-dependent renormalization function, $G(\Omega)$ is the generalized energy-dependent electron-boson coupling function averaged over the Fermi surface, μ^* is the screened Coulomb repulsion, $f(\omega)$ and $n(\omega)$ are the Fermi and Bose occupation factors, respectively, and $\beta = 1/k_B T$. Together, these equations form a nonlinear set of coupled integral equations which must be solved self-consistently for $\Delta(\omega,T)$.
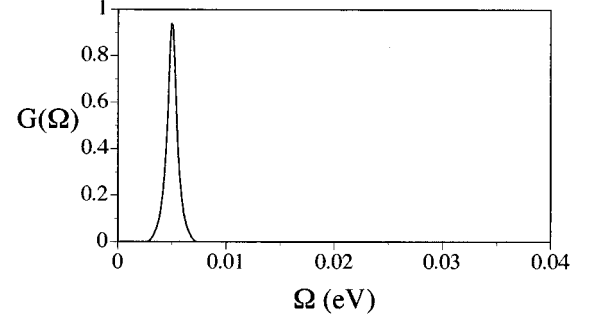

FIG. 1. The energy-dependent electron-boson coupling function used to illustrate the calculation procedures developed as a means of solving the finite-temperature real-energy-axis Eliashberg equations. The coupling function shown is a cutoff Lorentzian peak centered at 5.0 meV with a full width at half maximum of 1.0 meV.

An iterative procedure is typically used to solve such integral equations. If $G(\Omega)$, μ^*, and T are known, then a guess is made at the initial form of $\Delta(\omega,T)$. This first-order guess is usually taken as a constant, real quantity with a magnitude approximately that of a typical BCS gap. With this first-order guess of $\Delta(\omega,T)$, $Z(\omega,T)$ is calculated using Eq. (2). Then, a new $\Delta(\omega,T)$ is calculated using Eq. (1), the first-order guess at $\Delta(\omega,T)$, and the newly calculated $Z(\omega,T)$. This iteration procedure is repeated until the newly calculated $\Delta(\omega,T)$ does not differ significantly from the solution of the previous iteration.

III. ALGORITHM DESCRIPTION

In designing an efficient algorithm to calculate the solution of the Eliashberg equations it is useful to break down Eqs. (1) and (2) into individual computational tasks. These individual tasks may then be carried out by developing efficient integration procedures specific to each phase of the computation. The algorithm we have developed to solve the Eliashberg equations[24] can be divided into two major computational tasks; (1) evaluating $K_+(\omega,\omega',T)$ and $K_-(\omega,\omega',T)$, and (2) performing the iterative integrations necessary to obtain a self-consistent $\Delta(\omega,T)$. The former is complicated by the occurrence of simple poles along the axis of integration and the latter by the possible integrable singularities at energies near the superconducting gap edge. We will assume in the following development that $G(\Omega)$, T, and μ^* are known quantities.

For the purpose of illustrating the various portions of the algorithm, we set μ^* equal to zero and take $G(\Omega)$ to be a cutoff Lorentzian peak centered at 5.0 meV, with a full width at half maximum of 1.0 meV and an amplitude of 1.0. This electron-boson coupling spectrum is shown in Fig. 1. The cutoff Lorentzian line shape has been used historically to represent the energy-dependent electron-phonon interaction averaged over the Fermi surface.[15]

A. The evaluation of $K_+(\omega,\omega',T)$ and $K_-(\omega,\omega',T)$

One of the most important computational tasks is the accurate evaluation of the $K_+(\omega,\omega',T)$ and $K_-(\omega,\omega',T)$ integrals. These integrals are complicated by the fact that they contain both Fermi and Bose thermal occupation factors, in
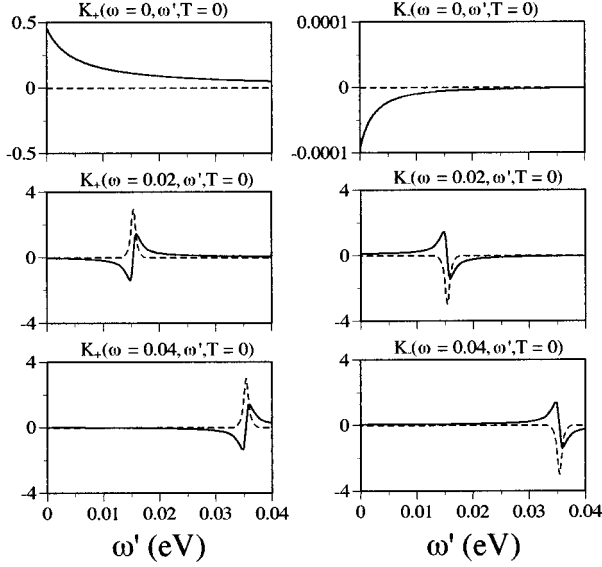
FIG. 2. The zero-temperature $K_{\pm}(\omega,\omega',T)$ calculated using the electron-boson coupling function of Fig. 1. The real (solid line) and imaginary (dashed line) components of these kernels are shown as a function of ω' for ω equal to 0, 0.02, and 0.04 eV.
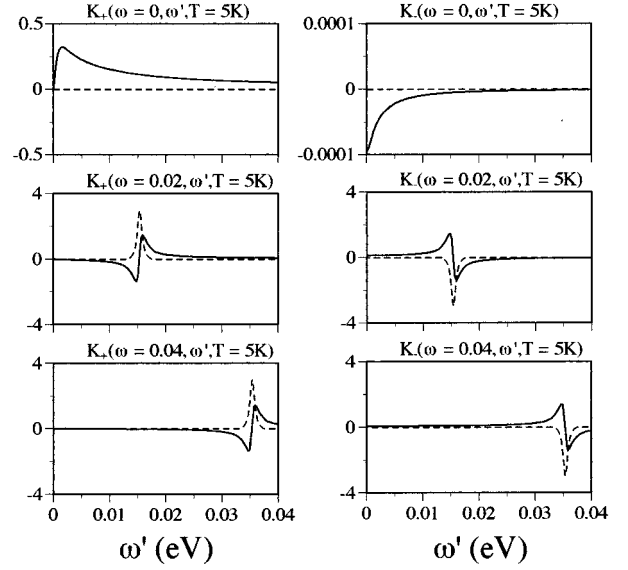

FIG. 3. The finite-temperature $K_{\pm}(\omega,\omega',T)$ calculated using the electron-boson coupling function of Fig. 1. The real (solid line) and imaginary (dashed line) components of these kernels are shown at $T=5$ K, as a function of ω' for ω equal to 0, 0.02, and 0.04 eV. The slight broadening of these functions with increased temperature is most noticeable in the $\omega=0$ kernel spectra.

addition to a number of simple poles which lie on the Ω energy axis. Although the literature implies that it is necessary to calculate these principal part integrals within each iteration cycle,[17] it is only necessary to evaluate these kernels *once* and store the values on an appropriate two-dimensional grid spanning all ω and ω'. Since $K_{+}(\omega,\omega',T)$ and $K_{-}(\omega,\omega',T)$ contain neither $\Delta(\omega,T)$ nor $Z(\omega,T)$, their values *do not change* during the iteration sequence, thus it is not necessary to reevaluate the kernels during the iterative procedure used to find the self-consistent solution, $\Delta(\omega,T)$. This feature dramatically reduces the time required to compute the solution.

We have named the procedure which calculates both $K_{+}(\omega,\omega',T)$ and $K_{-}(\omega,\omega',T)$ on a two-dimensional energy grid over $[\omega,\omega']$ the *initialization* stage. For each element $\{\omega,\omega'\}$ on this grid an integration over energy Ω is performed and the results are stored in a dynamically allocated memory location. Since $K_{+}(\omega,\omega',T)$ and $K_{-}(\omega,\omega',T)$ consist of both real and imaginary components, each $\{\omega,\omega'\}$ position generated during the *initialization* stage contains values for $\mathrm{Re}\{K_{+}(\omega,\omega',T)\}$, $\mathrm{Im}\{K_{+}(\omega,\omega',T)\}$, $\mathrm{Re}\{K_{-}(\omega,\omega',T)\}$, and $\mathrm{Im}\{K_{-}(\omega,\omega',T)\}$. By storing these quantities in a directly addressable memory location, these values may be accessed quickly during the subsequent iteration sequence.

The real and imaginary components of $K_{+}(\omega,\omega',T)$ and $K_{-}(\omega,\omega',T)$ evaluated using the electron-boson coupling spectrum of Fig. 1, are shown in Figs. 2 and 3. Figure 2 shows the zero-temperature real (solid line) and imaginary (dashed line) components of $K_{+}(\omega,\omega',T)$ and $K_{-}(\omega,\omega',T)$ evaluated at $\omega\sim0$ eV, $\omega=0.020$ eV, and $\omega=0.040$ eV. Figure 3 shows the same $K_{+}(\omega,\omega',T)$ and $K_{-}(\omega,\omega',T)$ evaluated at 5 K. The kernel functions can be seen to resemble the structure of the coupling function, $G(\Omega)$, in that there is a single peak (or derivative peak) structure which moves to higher ω' with higher values of ω. A+ finite temperatures

there is a small, but significant, change in the form of the kernel functions. In general, these functions tend to broaden slightly with temperature. This broadening is most easily seen in the finite temperature $K_{+}(\omega,\omega',T)$ and $K_{-}(\omega,\omega',T)$ spectra with $\omega\sim0$ eV in Fig. 3.

B. The iterative integration of the Eliashberg equations

With both the real and imaginary parts of $K_{+}(\omega,\omega',T)$ and $K_{-}(\omega,\omega',T)$ calculated and stored in memory, it is possible to calculate $\mathrm{Re}[Z(\omega,T)]$, $\mathrm{Im}[Z(\omega,T)]$, $\mathrm{Re}[\Delta(\omega,T)]$, and $\mathrm{Im}[\Delta(\omega,T)]$ given an initial guess at $\Delta(\omega,T)$. This part of the algorithm is referred to as the *iteration* stage. The *iteration* stage performs multiple integrations over the ω' variable in Eqs. (1) and (2) until a self-consistent $\Delta(\omega,T)$ is obtained. This process is complicated by the fact that the expressions

$$\mathrm{Re}\,\frac{\Delta(\omega',T)}{\sqrt{\omega'^2-\Delta^2(\omega',T)}} \qquad (5)$$

and

$$\mathrm{Re}\,\frac{\omega'}{\sqrt{\omega'^2-\Delta^2(\omega',T)}}, \qquad (6)$$

which appear in Eqs. (1) and (2) *may* possess integrable singularities at energies approximately equal to the superconducting gap edge Δ_0, defined as $\mathrm{Re}\{\Delta(\omega,T)\}$ at $\omega=\mathrm{Re}\{\Delta(\omega\sim0,T)\}$.[4] More explicitly, Δ_0 is defined as the magnitude of the real part of $\Delta(\omega,T)$ evaluated at energy ω equal to the real part of $\Delta(\omega,T)$ at energy $\omega\sim0$, and temperature, T. To accommodate this singular portion of the integral, which will necessarily shift in energy with each iteration cycle until self-consistency is achieved, we have developed a

singularity integration routine. This routine dynamically adjusts the integration grid such that an accurate evaluation of the singular part of the integral can be obtained.

Because the integrals involved in the *iteration* stage do not contain any problematic regions except for the region near the possible singularity, the remaining portion of the iterative integration is rapidly evaluated using standard integration procedures. In this algorithm, sufficient accuracy and speed are obtained by using the trapezoidal rule in all regions of the integration over ω' where the *singularity integration* procedures are not required.

C. The full calculation sequence

The outline of the complete sequence of calculations involved in obtaining $\Delta(\omega,T)$ based upon the $G(\Omega)$ shown in Fig. 1 is as follows. In this example we take both T and μ^* equal to zero. With these definitions of $G(\Omega)$, μ^*, T, and the upper-energy cutoff limit set to 0.04 eV, the *initialization* stage calculates $K_+(\omega,\omega',T)$ and $K_-(\omega,\omega',T)$, and stores these values on a two-dimensional grid of $[\omega,\omega']$. Then, the zeroeth-order guess at $\Delta(\omega,T)$ is defined as a real, energy-independent BCS gap. This guess is taken to be 0.5 meV and is shown as the BCS $\Delta(\omega)$ in Fig. 4, where the solid and dashed lines are the real and imaginary components of $\Delta(\omega,T)$, respectively. With this zeroeth-order definition of $\Delta(\omega,T)$ and $K_-(\omega,\omega',T)$, a first-order $Z(\omega,T)$ is calculated using Eq. (2).[25] With this newly calculated $Z(\omega,T)$, $K_+(\omega,\omega',T)$, and the zeroeth-order guess at $\Delta(\omega,T)$, a new $\Delta(\omega,T)$ is calculated using Eq. (1). This $\Delta(\omega,T)$ is shown as the first iteration in Fig. 4, where it can be seen that even after a single iteration there is considerable structure in the functional form of $\Delta(\omega,T)$. Successive iterations of these equations leads to the self-consistent $\Delta(\omega,T)$. A complete iteration sequence is shown in Fig. 4 where $\Delta(\omega,T)$ is plotted after 1, 2, 4, 10, and 15 iterations. Typically, $\Delta(\omega,T)$ converges to within 1% in less than 20 iterations. In the sequence shown in Fig. 4, $\Delta(\omega,T)$ has converged to within 5% by the 10th iteration and to within 0.5% by the 15th.

IV. RESULTS

Having developed a fast, convenient means of solving the Eliashberg equations for arbitrary $G(\Omega)$, T, and μ^*, several model systems have been studied and the representative $\Delta(\omega,T)$ obtained. In the following section, we illustrate the reduction of the magnitude of $\Delta(\omega,T)$ due to a finite μ^*, the differences between a weak- and strong-coupling $\Delta(\omega,T)$ at zero and finite temperatures, and how the spectral form of $G(\Omega)$ affects the superconducting critical temperatures of Eliashberg superconductors.

A. The effects of a finite screened Coulomb repulsion, μ^*

In phonon-mediated superconductivity, the repulsive potential normally experienced between the electrons in the material is overcome by an effective attractive potential due to the retarded interaction of the electrons with the phonons. Calculations which took into account both the instantaneous Coulomb repulsion μ^* and the retarded electron-phonon interaction were carried out by Morel and Anderson in 1962.[18] These calculations lead to similar results obtained by
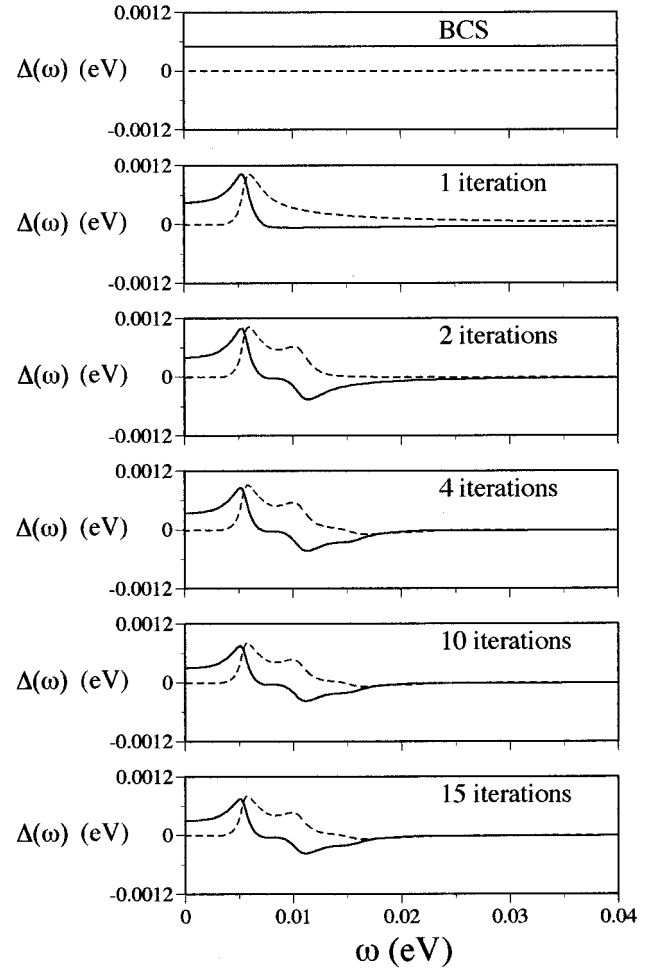

FIG. 4. The real (solid line) and imaginary (dashed line) components of the zero-temperature $\Delta(\omega)$ calculated during the *iteration* stage using the coupling function of Fig. 1. A BCS gap is used as the zeroeth-order guess at $\Delta(\omega)$. The sequence continues to iterate until the previously calculated $\Delta(\omega)$ is not significantly different from the results of the latest iteration. In this example, $\Delta(\omega)$ has converged to within 5.0% of its final value by the tenth iteration and to within 0.5% by the 15th.

Bogoliubov[26] which included both a Coulomb repulsion term and a BCS-like pairing interaction. In BCS theory, the pairing interaction $N(0)V$ is taken to be instantaneous and results in an energy-independent superconducting gap.[2] In the weak-coupling BCS limit of Eliashberg theory, the BCS pairing interaction can be written as

$$N(0)V = \frac{\lambda - \mu^*}{1 + \lambda}, \qquad (7)$$

where λ is defined as[20]

$$\lambda = 2 \int_0^\infty \frac{d\omega}{\omega} G(\omega), \qquad (8)$$

μ^* is defined as[18]

$$\frac{1}{\mu^*} = \frac{1}{\mu} + \ln\left(\frac{\omega_{el}}{\omega_{ph}}\right), \qquad (9)$$
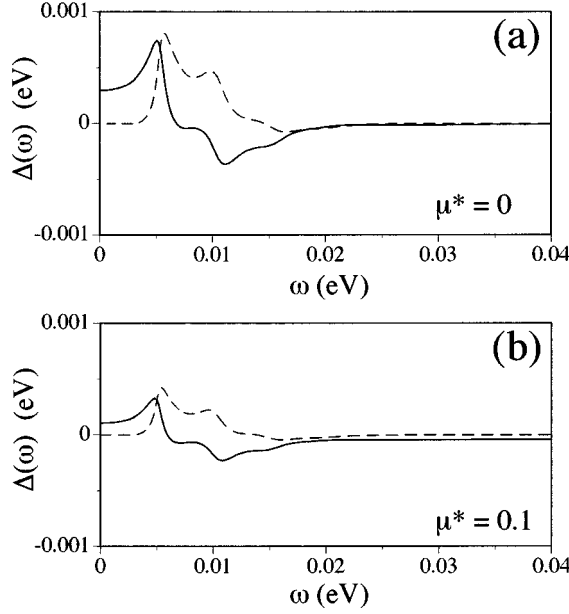
FIG. 5. The real (solid line) and imaginary (dashed line) components of the zero-temperature $\Delta(\omega)$ based upon the $G(\Omega)$ of Fig. 1. (a) $\Delta(\omega)$ obtained with μ^* set equal to zero. (b) $\Delta(\omega)$ obtained with μ^* equal 0.1. In addition to the overall reduction in the magnitude of $\Delta(\omega)$ with finite μ^*, there is also a constant negative component of $\Delta(\omega)$ at high energies reflecting the energy-independent Coulomb repulsion of the electrons.

where $N(0)$ is the single spin density of electronic states at the Fermi energy, V is the BCS pairing potential, ω_{el} is the plasma frequency, and ω_{ph} is the Debye energy of the material. Thus, it can be seen from the form of Eq. (9), that the magnitude of μ^* is dramatically reduced from the instantaneous Coulomb repulsion μ by the difference in propagation times of the electron-electron and the electron-phonon interaction.[13] Typical values of μ^* fall between 0.1 and 0.2 eV.

The inclusion of a finite μ^* in the solution of the Eliashberg equations results in two dramatic changes in the form of $\Delta(\omega,T)$. The most obvious of these is the direct reduction in the real part of $\Delta(\omega,T)$ as seen in Eq. (1). This reduction in the magnitude of $\Delta(\omega,T)$ also reduces the T_c of the model. The second, less obvious effect is that the real part of $\Delta(\omega,T)$ is nonzero at high energies.[4] This high-energy component of $\Delta(\omega,T)$, though repulsive, is finite and independent of energy due to the energy-independent Coulomb repulsion of the electrons. This phenomena is illustrated in Fig. 5 where the solid and dashed lines indicate the real and imaginary components of $\Delta(\omega)$, respectively. The $G(\Omega)$ of Fig. 1 was used for these zero-temperature calculations. Figures 5(a) and 5(b) show the resulting $\Delta(\omega,T=0)$ for the model with μ^* equal to zero and μ^* equal to 0.1, respectively. In Fig. 5(a) there is the usual structure in $\Delta(\omega,T=0)$ which reflects the structure of $G(\Omega)$. But at approximately four times the energy of the peak in $G(\Omega)$, $\Delta(\omega,T=0)$ is seen to be zero. When μ^* is finite, however, in addition to the overall reduction in magnitude of $\Delta(\omega,T=0)$, the real part of $\Delta(\omega,T=0)$ is finite and negative at high energies. This can be seen to arise from the form of Eq. (1) where μ^* only directly affects the real part of

$\Delta(\omega,T)$. The imaginary part of $\Delta(\omega,T)$ is indirectly changed by the finite μ^* through the self-consistency and causality restrictions of the theory.

Although the magnitude of μ^* plays a significant role in Eliashberg theory, the experimental determination of this quantity with precision is difficult. McMillan and Rowell[5] determined μ^* by allowing its magnitude to vary as a floating parameter in the inversion of $N/I/S$ tunneling data. Ultimately, the magnitude of μ^* is determined in this method by matching the experimentally determined Δ_0, with a theoretical Δ_0 obtained from a trial $\alpha^2(\Omega)F(\Omega)$ and the floating μ^* parameter.[27] Since the resulting magnitude of Δ_0 is a strong function of the magnitude of μ^*, as can be seen from the form of Eq. (1), the determination of the magnitude of the Coulomb repulsion by this method is not very precise. A better inversion method has been developed by Galkin et al.[28] in which the magnitude of μ^* is not required during the inversion procedure used to obtain $\alpha^2(\Omega)F(\Omega)$ from tunneling data. In this method, the magnitude of μ^* is calculated analytically after $\alpha^2(\Omega)F(\Omega)$ has been determined.

B. Weak- versus strong-coupling $\Delta(\omega,T)$

The distinction between weak- and strong-coupling superconductors is not clear cut, but in general is characterized by the value of the ratio $2\Delta_0(T=0)/k_BT_c$. In weak-coupling BCS superconductors this ratio is approximately 3.52, but in strong-coupling materials, such as lead and mercury, it is higher. In addition, strong-coupling superconductors possess an electron-phonon coupling strength large enough that there are observable changes at the phonon energies in the measured superconducting density of states defined by[15]

$$N_S(\omega) = N_N(\omega)\text{Re}\left(\frac{\omega}{\sqrt{\omega^2 - \Delta^2(\omega)}}\right), \qquad (10)$$

where $N_S(\omega)$ and $N_N(\omega)$ are the energy-dependent density of states of the materials. In strong-coupling superconductivity, the structure in $\Delta(\omega,T)$ is large enough that there are observable variations in $N_S(\omega)$ at energies corresponding to the analogous structure in $G(\Omega)$. However, even in the weak-coupling limit of Eliashberg theory, there is considerable structure in the associated $\Delta(\omega,T)$. Unfortunately, experimental evidence of this type of structure in the gap is difficult to obtain because of the small magnitude of the gap. Thus in weak-coupling superconductors, in the absence of other high precision data, the BCS approximation is commonly used to describe the observed experimental quantities.

In the interpretation of experiments such as the temperature dependence of the spin-lattice relaxation rate,[29,30] the thermodynamic critical magnetic field,[31] the London penetration depth,[32] and the electronic specific heat of a superconductor,[33,34] it is important to use the proper form of $\Delta(\omega,T)$ because these quantities are evaluated by integrating $\Delta(\omega,T)$ over energy, ω. Thus, the changes in the functional form of $\Delta(\omega,T)$ which arise from the magnitude of the coupling involved may be important in the interpretation.

To illustrate this we have calculated $\Delta(\omega,T)$ in both the weak- and strong-coupling limits of Eliashberg theory. The model parameters and results of these calculations are shown in Table I. Model A is a weak-coupling electron-phonon

TABLE I. Weak- and strong-coupling model parameters, along with the critical temperature T_c and magnitude of the gap edge at zero temperature Δ_0 obtained from finite-temperature Eliashberg calculations. A_0, ω_0, and Γ_0 are the parameters used to describe the amplitude, energy, and width of the cutoff Lorentzian peak used to model the electron-boson coupling function. T_c^{AD} is the approximate critical temperature of the model obtained from the Allen and Dynes analytic expression for T_c [Eq. (11)]. This approximate T_c is obtained from the magnitude of the effective Coulomb repulsion μ^*, the integrated coupling strength λ, and the logarithmic moment of the electron-boson coupling spectrum $\omega_{\ln}$.

Model	A_0	ω_0 (meV)	Γ_0 (meV)	μ^*	λ	$\omega_{\ln}$ (meV)	T_c^{AD} (K)	T_c (K)	Δ_0 (meV)	$2\Delta_0/kT_c$
A	1.0	5.0	0.5	0.0	0.458	4.8	1.71	1.83	0.295	3.74
B	2.0	5.0	0.5	0.0	0.916	4.8	5.30	6.05	1.064	4.08

model with a $2\Delta_0(T=0)/k_B T_c$ ratio of 3.74, this is close to the BCS limit of 3.52. The resulting real (solid) and imaginary (dashed) components of $\Delta(\omega,T)$ based upon this coupling model are shown in Fig. 6(a) in reduced coordinates $\Delta(\omega,T)/\Delta_0(T=0)$ versus $[\omega-\Delta_0(T=0)]/\omega_0$ where ω_0 is energy of the Lorentzian peak used as the electron-phonon coupling function. The gap function is plotted this way to allow for a direct comparison of the weak-coupling $\Delta(\omega,T)$ with the strong-coupling $\Delta(\omega,T)$ shown in Fig. 6(b), because the structure in $\Delta(\omega,T)$ which results from the form of $G(\Omega)$ is located at $\omega_0+\Delta_0(T)$ in the $\Delta(\omega,T)$ spectrum.[4] The strong-coupling $\Delta(\omega,T)$ is seen to have much more structure at multiples of ω_0 even at zero temperature. Clearly, this additional structure in the functional form of $\Delta(\omega,T)$ will effect the interpretation of experiments.

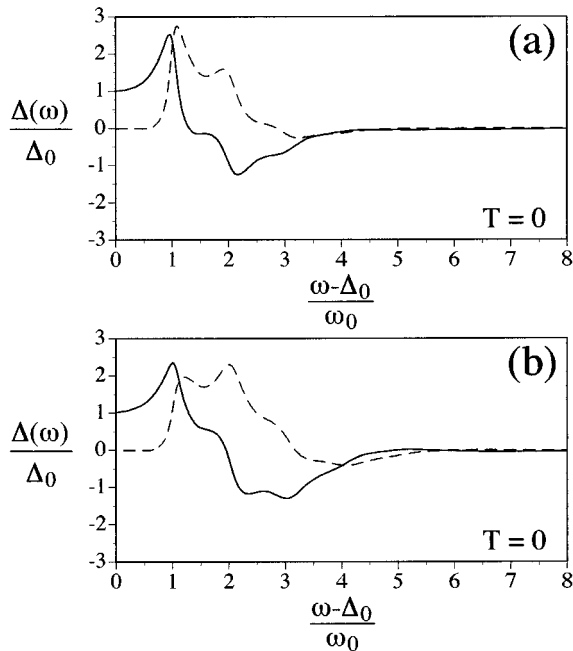Although the differences in the form of $\Delta(\omega,T)$ are rather subtle at low temperature, they become quite pronounced at higher temperatures, particularly at temperatures near T_c. In these instances, it is important to incorporate the finite-temperature characteristics of Eliashberg theory into the interpretation of the experimental results. In Fig. 7 we show $\Delta(\omega,T)$ of the model coupling spectra in the weak- and strong-coupling limit at $T=0.9T_c$. The difference in the functional form of the two Eliashberg gap functions is quite dramatic. While it is true that the weak-coupling $\Delta(\omega,T)$ may be well approximated by multiplying the zero temperature solution by the known temperature dependence of the BCS gap [compare Figs. 6(a) and 7(a)], this approximation clearly breaks down in the strong-coupling case shown in Fig. 7(b). The strong-coupling $\Delta(\omega,T)$, in addition to having pro-

FIG. 6. The real (solid line) and imaginary (dashed line) components of the zero-temperature $\Delta(\omega)$, plotted in reduced coordinates, based upon the parameters shown in Table I. (a) The weak-coupling $\Delta(\omega)$ obtained from the parameters defined by Model A in Table I. (b) The strong-coupling $\Delta(\omega)$ obtained from the parameters defined by Model B in Table I. The strong-coupling $\Delta(\omega)$ is seen to possess much more structure than the weak-coupling $\Delta(\omega)$ at the harmonics of the peak in $G(\Omega)$, ω_0.
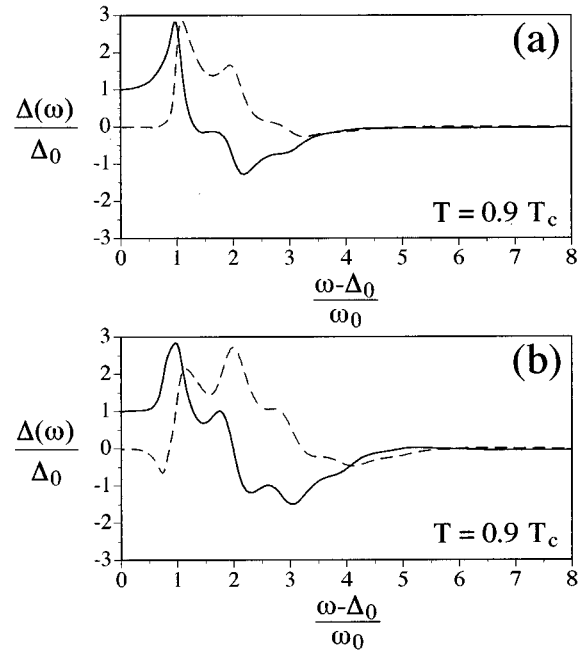

FIG. 7. The real (solid line) and imaginary (dashed line) components of $\Delta(\omega)$ at $T=0.9T_c$, plotted in reduced coordinates, based upon the parameters shown in Table I. (a) The weak-coupling $\Delta(\omega)$ at $T=0.9T_c$ obtained from the parameters defined by Model A in Table I. (b) The strong-coupling $\Delta(\omega)$ at $T=0.9T_c$ obtained from the parameters defined by Model B in Table I. While the finite-temperature weak-coupling $\Delta(\omega)$ plotted in these reduced coordinates is virtually identical to the zero-temperature solution, there are significant differences between the zero- and finite-temperature $\Delta(\omega)$ in the strong-coupling limit. One distinct difference is the appearance of the negative peak in the Im$\{\Delta(\omega)\}$ at energies below ω_0.

nounced structure at harmonics of ω_0, also possesses a large negative imaginary part of $\Delta(\omega,T)$ at low energies. In certain instances, this structure may result in what is commonly referred to as gapless superconductivity. This is not because there is no $\Delta(\omega,T)$, but rather because there is no well defined Δ_0 in the superconducting density of states. That is, there appear to be states at energies below the gap edge. These contributions below Δ_0 arise from the form of $\Delta(\omega,T)$ and are a natural result of finite-temperature Eliashberg theory. Physically, they arise from the recombination of thermally excited quasiparticle states with the emission of phonons near the gap edge. This process is reflected in the negative peak in the imaginary part of $\Delta(\omega,T)$ at energies below ω_0. This phenomenon can lead to the loss of certain coherence properties commonly associated with a BCS superconducting state. In particular, the absence of the Hebel-Slichter peak[35,36] in the nuclear-spin-relaxation rate can be attributed to the finite-temperature form of $\Delta(\omega,T)$,[29,30] and not necessarily to exotic electron pairing mechanisms.

In addition to significant differences in the functional form of the weak- and strong-coupling $\Delta(\omega,T)$, there are also similar differences in the weak- and strong-coupling $Z(\omega,T)$. Although mass renormalization effects are unimportant in the interpretation of many experiments, the form of $Z(\omega,T)$ must be taken into account, for example, when evaluating measurements of the discontinuity in the electronic specific heat at T_c,[33,34] the temperature dependence of the thermodynamic critical field,[31] and the temperature dependence of the London penetration depth.[37]

To illustrate the difference in $Z(\omega,T)$ in the weak- and strong-coupling limits of Eliashberg theory, we plot in Fig. 8 both the real (solid) and imaginary (dashed) components of $Z(\omega,T)$ versus $[\omega-\Delta_0(T=0)]/\omega_0$ for the model systems of Table I. The zero-temperature renormalization function, in the weak- and strong-coupling limits, is shown in Figs. 8(a) and 8(b), respectively. It is seen that, except for the increase in magnitude of $Z(\omega,T)$ in the strong-coupling case, the two renormalization functions are quite similar. In each case, the function peaks at approximately ω_0 and tends to either unity [Re$\{Z(\omega,T)\}$] or zero [Im$\{Z(\omega,T)\}$] at high ω.

Figure 9 shows that, as with $\Delta(\omega,T)$ at higher temperatures, there are dramatic differences in the weak- and strong-coupling $Z(\omega,T)$ at temperatures near T_c. The respective weak- and strong-coupling $Z(\omega,T)$ at $0.9T_c$ are shown in Figs. 9(a) and 9(b). While the finite-temperature weak-coupling $Z(\omega,T)$ shown in Fig. 9(a) is essentially the same as the zero-temperature case [Fig. 8(a)] the strong-coupling $Z(\omega,T)$ shows additional structure at low energies. Again, this structure reflects phonon emission processes which can occur at finite temperatures. This structure in $Z(\omega,T)$ should be taken into account in the interpretation of experiments whose results are influenced by renormalization effects, such as those discussed above.

C. Calculations of the superconducting critical temperature

One of the distinct advantages of having an efficient algorithm available to calculate $\Delta(\omega,T)$ for arbitrary $G(\Omega)$, μ^*, and T, is that it can be used to aid in the interpretation of experiments beyond the usual BCS model. A self-consistent check of a proposed model $G(\Omega)$ is that it accurately reproduce the measured T_c. With this algorithm, the T_c of any
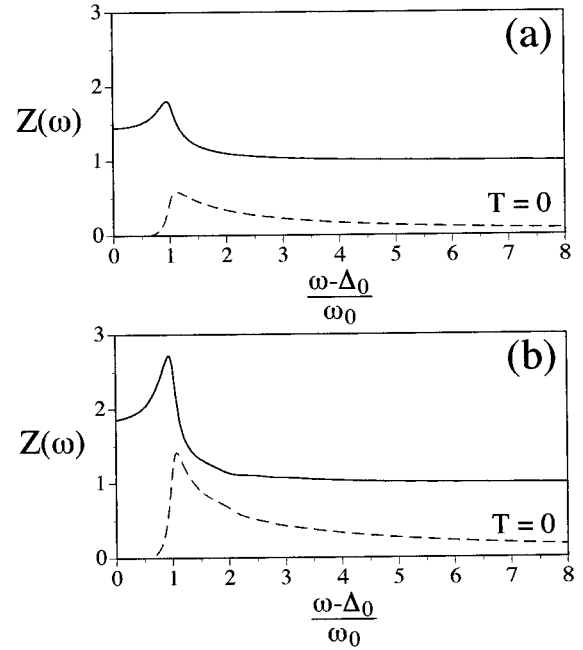

FIG. 8. The real (solid line) and imaginary (dashed line) components of the zero-temperature $Z(\omega)$, plotted in reduced coordinates, based upon the parameters shown in Table I. (a) The weak-coupling $Z(\omega)$ obtained from the parameters defined by Model A in Table I. (b) The strong-coupling $Z(\omega)$ obtained from the parameters defined by Model B in Table I. Except for the difference in the magnitude of the coupling, both of these functions are quite similar. In general, $Z(\omega)$ displays peaks at energies near the peak of the underlying electron-boson coupling function.

model can be calculated accurately without having to resort to approximate analytic expressions for the critical temperature. In 1968, McMillan[20] formulated an analytic expression for T_c given λ, μ^*, and the average phonon frequency $\langle\omega\rangle$. The McMillan formula was extended by Allen and Dynes in 1975,[13] with the main difference being the replacement of the $\langle\omega\rangle$ prefactor with the logarithmic moment of the phonon spectrum, ω_{ln}. The analytic expression formulated by Allen and Dynes is the most common formula used to calculate approximate critical temperatures. It is usually written as

$$k_B T_c = \frac{\hbar\omega_{ln}}{1.2}\exp\left(-\frac{1.04(1+\lambda)}{\lambda-\mu^*(1+0.62\lambda)}\right), \quad (11)$$

with

$$\omega_{ln} = \exp\left(\frac{2}{\lambda}\int_0^\infty\frac{d\omega}{\omega}G(\omega)\ln(\omega)\right), \quad (12)$$

and μ^* and λ defined by Eqs. (8) and (9), respectively. Although this expression is reasonably accurate as a preliminary estimate for the superconducting critical temperature, the T_c calculated with this expression is inadequate to describe many experiments because of an approximately 15% uncertainty.[14] Because critical temperatures are routinely measured with a precision better than 1%, the Allen and Dynes analytic expression for T_c is not accurate enough to explain the temperature-dependent effects observed in many experiments.
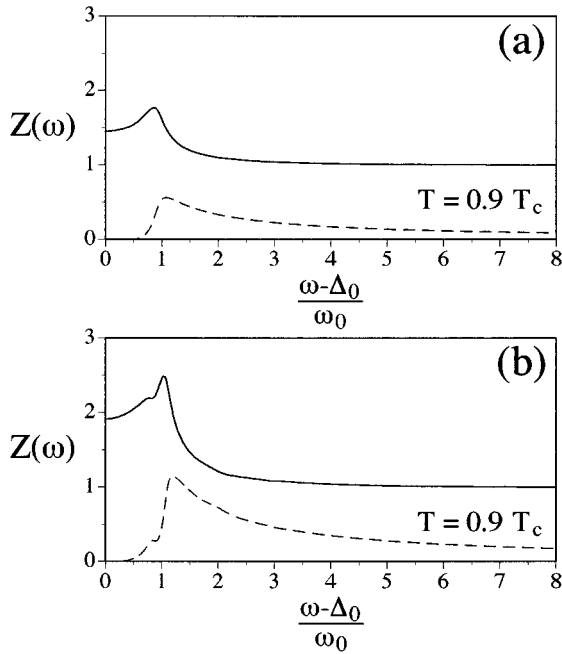
FIG. 9. The real (solid line) and imaginary (dashed line) components of $Z(\omega)$ at $T = 0.9T_c$, plotted in reduced coordinates, based upon the parameters shown in Table I. (a) The weak-coupling $Z(\omega)$ at $T = 0.9T_c$ obtained from the parameters defined by Model A in Table I. (b) The strong-coupling $Z(\omega)$ at $T = 0.9T_c$ obtained from the parameters defined by Model B in Table I. Similar to the weak-coupling $\Delta(\omega)$, the finite-temperature weak-coupling $Z(\omega)$ plotted in these reduced coordinates is virtually identical to the zero-temperature $Z(\omega)$. The strong-coupling $Z(\omega)$ at finite temperatures, however, is seen to possess additional structure at energies below the peak in $G(\Omega)$.

The superconducting critical temperature is the temperature at which $\Delta(\omega, T)$ equals zero. Thus, we can find T_c for a model $G(\Omega)$ and μ^* by solving for $\Delta(\omega, T)$ at a variety of temperatures and find the temperature at which $\Delta(\omega, T)$ collapses to zero. This is illustrated in Fig. 10 for the model $G(\Omega)$ shown in Fig. 1, where we show the real [Fig. 10(a)] and imaginary [Fig. 10(b)] components of $\Delta(\omega, T)$ at temperatures up to 2 K. The T_c is determined by plotting Δ_0 at each temperature and, for the weak-coupling models, fitting the data to the temperature dependence of a BCS gap.[2,38] The temperature dependence of Δ_0 for this model is shown in Fig. 11, where the solid line represents the BCS temperature-dependent gap. The critical temperature of this model was determined to be 1.83 K.

We have calculated T_c for a number of electron-phonon coupling functions[39] with μ^*, equal to zero and 0.15. For each model, the zero-temperature $\Delta(\omega, T)$ is calculated, then higher temperature solutions are obtained until T_c can be determined from the characteristic collapse of Δ_0. We find that T_c can usually be obtained accurately by calculating $\Delta(\omega, T)$ at four or five different temperatures. In Fig. 12 we plot $T_c/\omega_{\ln}$ versus λ for these model solutions, along with the Allen and Dynes analytic expression for T_c.[13] We find good agreement between these results for a variety of forms of $G(\Omega)$ indicating that the $\omega_{\ln}$ prefactor describes well the energy dependence of the coupling function for λ less than approximately 0.75. At higher values of λ, there is a signifi-
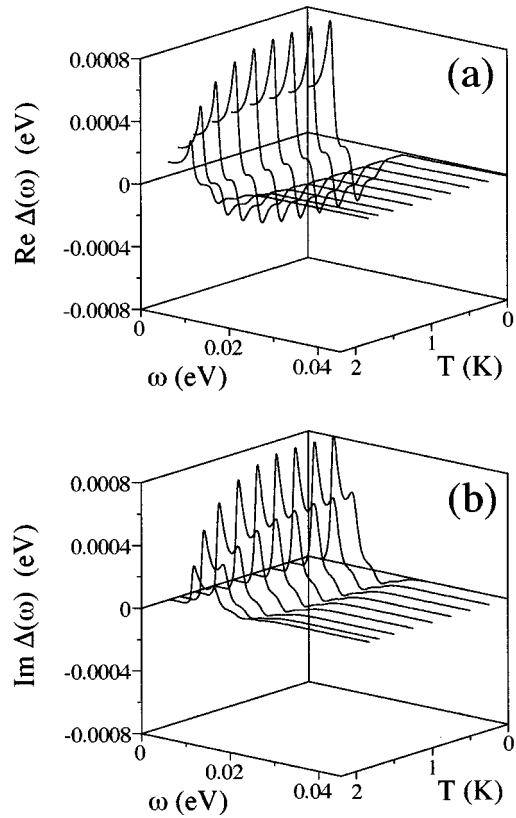

FIG. 10. The full temperature dependence of $\Delta(\omega)$ based upon the $G(\Omega)$ in Fig. 1. (a) The real part of $\Delta(\omega)$ versus temperature. (b) The imaginary part of $\Delta(\omega)$ versus temperature. The T_c of the model is obtained by finding the temperature at which $\Delta(\omega)$ collapses to zero.

cant deviation between our results and the Allen and Dynes expression for T_c, and that for a given $\omega_{\ln}$, in general, the analytic expression for T_c yields a lower value than the actual T_c. Because this error in the value of the critical tem-
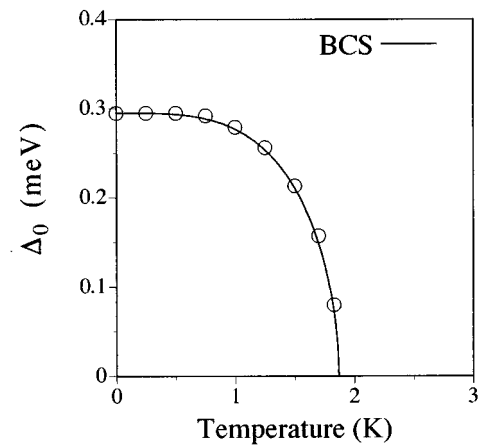

FIG. 11. The temperature dependence of the superconducting gap edge based upon the $G(\Omega)$ in Fig. 1. The T_c is obtained by fitting the temperature-dependent magnitude of Δ_0 ($\bigcirc$) to the known temperature dependence of the BCS gap function. The T_c of this model was determined to be 1.83 K using this procedure.
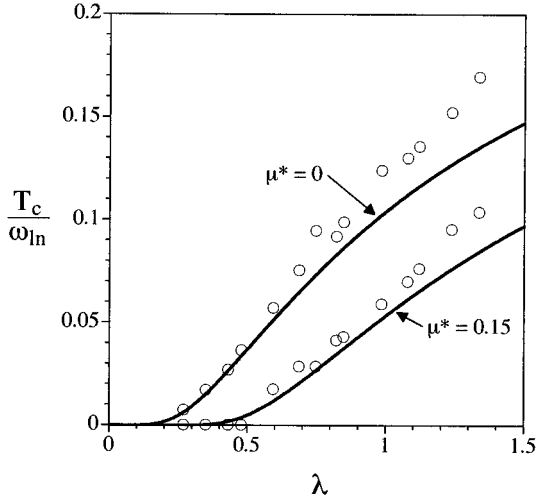
FIG. 12. $T_c/\omega_{\ln}$ versus λ for a variety of forms of $G(\Omega)$. The open circles (○) represent the results obtained by calculating the T_c of the model using the full finite-temperature Eliashberg equations, and finding the temperature at which Δ_0 collapses to zero. The solid line represents the approximate analytic expression for T_c derived by Allen and Dynes.
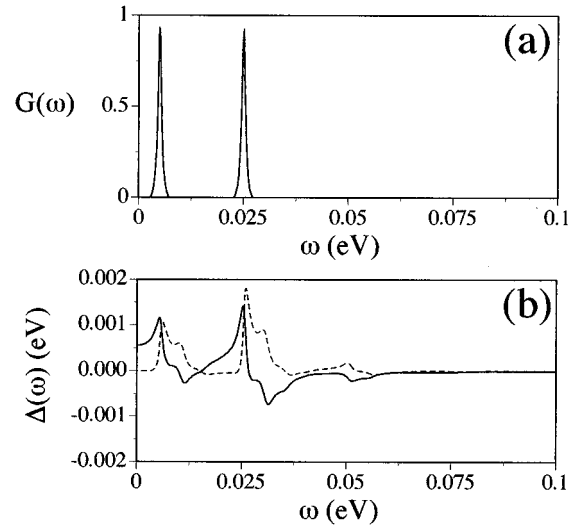

FIG. 13. The joint electron-phonon based pairing mechanism. (a) A model $G(\Omega)$ consisting of two well separated regions of significant coupling strength. (b) The zero-temperature $\Delta(\omega)$ obtained using the $G(\Omega)$ in (a). The parameters and results of these calculations are shown in joint electron-phonon coupling section of Table II.

perature increases dramatically for values of λ greater than 0.75, the full finite-temperature calculation must be carried out when comparing the results of Eliashberg theory to experiment with materials of moderate- to strong-coupling strength.

D. The two-component electron-boson coupling spectrum

A particularly interesting form of the electron-boson coupling spectrum is one in which there are two distinct energy regions where there is significant coupling strength. This type of coupling spectrum is referred to as the joint mechanism of superconductivity.[14] There are many examples of superconducting materials which possess this general type of electron-boson coupling spectrum. These include elemental metals such as lead and indium,[5] Nb_3Sn, Nb_3Al, and other $A15$ materials,[40] and NbN and other refractory materials[41] which possess significant electron-phonon coupling strength at both low and high regions of the phonon spectrum. More recently, this type of mechanism has been suggested as the operative mechanism of superconductivity in the K_3C_{60} materials,[42,43] where there may be both low-energy intersphere, as well as high-energy intrasphere vibrational modes which are responsible for the pairing.

We first consider the generalized joint electron-phonon coupling function shown in Fig. 13(a). The zero-temperature $\Delta(\omega,T)$ of this model is shown in Fig. 13(b), where it is seen that there is considerable structure in $\Delta(\omega,T)$ at energies between the peaks in $G(\Omega)$. Using procedures outlined in the previous section we calculate the T_c of this model system to be approximately 3.48 K. The significance of this form of $G(\Omega)$ is dramatically illustrated when we decompose the coupling into single-peak coupling functions and calculate the critical temperatures of each individual peak. The parameters used in these calculations, and the results are given in Table II. From these results it is apparent that if the high-

energy coupling is neglected, the T_c of the model drops to 1.83 K, a reduction of nearly a factor of 2. Alternatively, if the low-energy contribution to $G(\Omega)$ is neglected, the model is not superconducting *at any temperature*. It is a remarkable, unexpected consequence of Eliashberg theory that the inclusion of a very weak, high-energy coupling would be so effective in raising the T_c of the model. While it has been known for many years that any increase in the amplitude of $G(\Omega)$ will result in an increase in the T_c of the material,[44,45] it was not clear how the *spectral form* of a given $G(\Omega)$ could enhance T_c. It is clear from these results that there is a dramatic enhancement of the superconducting critical temperature with the inclusion of the weakly coupled high-energy interaction in $G(\Omega)$. We find that this is a general result of Eliashberg theory, that is, that the sum of the critical temperatures of the individual components of a joint coupling function is always less than the T_c of the full $G(\Omega)$.

This joint electron-boson coupling function approach can be further extended to describe the results of Eliashberg theory based upon a model interaction which consists of both an electron-phonon interaction and a high-energy electronic electron-boson interaction. We have found that this model is required in the interpretation of recently measured optical data. We have previously reported the results of a series of optical experiments where we measured the superconducting–normal-state reflectance ratio (R_S/R_N) of $Tl_2Ba_2Ca_2Cu_3O_{10}$, $Tl_2Ba_2CaCu_2O_8$, $(BiPb)_2Sr_2Ca_2Cu_3O_{10}$, and $YBa_2Cu_3O_7$ for photon energies between 0.3 and 5.0 eV.[9,10] We interpreted the experimental data using finite-temperature Eliashberg theory and the strong-coupling extension of Mattis-Bardeen theory developed by Nam.[46,47] The results indicate that the operative electron-boson coupling spectrum of these materials consists of both an electron-phonon component and a high-energy electron-boson component located between 1.6 and 2.1 eV.

TABLE II. Results of finite-temperature Eliashberg calculations based upon a two-component electron-boson coupling spectrum. The parameters in the table are defined in Table I.

Model	A_0	ω_0 (eV)	Γ_0 (eV)	A_1	ω_1 (eV)	Γ_1 (eV)	μ^*	λ	ω_{ln} (eV)	T_c^{AD} (K)	T_c (K)	Δ_0 (meV)	$2\Delta_0/kT_c$
Joint	1.0	0.005	0.0005	1.0	0.025	0.0005	0.0	0.549	0.0063	3.26	3.48	0.555	3.70
e-ph	1.0	0.005	0.0005				0.0	0.458	0.0048	1.70	1.83	0.295	3.74
coupling				1.0	0.025	0.0005	0.0	0.090	0.0248	0.0	0.0	0.0	
Joint	1.9	0.050	0.007	0.835	1.60	0.20	0.15	1.495	0.1003	112.9	118.1	24.4	4.80
HTS	1.9	0.050	0.007				0.15	1.134	0.0461	35.7	44.8	8.657	4.49
coupling				0.835	1.60	0.20	0.15	0.361	1.563	5.23	20.5	4.723	5.34

An electron-boson coupling function consisting of both an electron-phonon component and a high-energy electronic electron-boson component has been suggested as a possible mechanism for high-T_c superconductivity.[48,49] The basic idea of the model is that the T_c of a superconductor may be raised by increasing the energy of the interaction which mediates the pairing of the electrons. This was suggested by Little in the context of organic superconductors,[50] then later by Ginzburg,[51] and by Allender, Bray, and Bardeen,[52] in the context of layered systems,[8] and has been refined through the years.[53] In the following model calculations we extend the joint electron-phonon coupling spectrum of the previous section to include both an electron-phonon interaction and an electronic electron-boson interaction. Implicit to these calculations is the assumption that Eliashberg theory is an appropriate framework within which to describe the superconductivity of this model. Furthermore, we neglect any effects of anisotropy although these are known to be a significant factor in the cuprate superconductors.

The generalized coupling function used in these calculations and the resulting $\Delta(\omega,T)$ calculated at zero temperature are shown in Fig. 14. Note the expanded ω scale from zero to 0.5 eV. The parameters used in these calculations, and the results of the finite-temperature calculations, are shown under the joint high-temperature superconductivity (HTS) coupling section of Table II. Both of the peaks in this coupling function are described by cutoff Lorentzians. Figure 14(a) shows the $G(\Omega)$ of this model which consists of a broad electron-phonon component centered at 50 meV and a high-energy electron-boson component centered at 1.6 eV. The zero-temperature $\Delta(\omega)$ based upon this model interaction is shown in Fig. 14(b). As in the joint electron-phonon based interaction, there is significant structure in $\Delta(\omega)$ at energies between the peaks of $G(\Omega)$. Specifically, the real part of $\Delta(\omega)$, although slightly negative at energies immediately above the phonon energies, is positive and nearly constant up to approximately 0.5 eV. This feature will manifest itself in a negative magnitude of μ^* obtained from the inversion of tunneling spectra.[14] This arises because typical tunneling experiments only probe energies up to approximately 100 meV. Thus, a negative μ^* implies the existence of a higher-energy component of the electron-boson coupling function which is, necessarily, compatible with the electron-phonon interaction.

The critical temperatures of the full $G(\Omega)$, and the individual components of $G(\Omega)$, for this model are shown in Table II. As in the joint electron-phonon based interaction, the inclusion of the high-energy component of the coupling function is dramatic. The T_c of the purely electron-phonon based interaction is calculated to be 44.8 K, while that of the high-energy electron-boson interaction is 20.5 K. The full $G(\Omega)$, however, has a critical temperature of 118.1 K, similar to the observed T_c of the cuprate superconductors. Again, the T_c of the full $G(\Omega)$ is much greater than the sum of its individual components.

This result demonstrates the importance of the electron-phonon interaction in high-temperature superconductivity. The overall conclusion is that a very modest coupling interaction at high energy, in addition to a moderate electron-phonon interaction, can give rise to critical temperatures of the order of 100 K.[54] This mechanism is slightly different from previously proposed theories of high-temperature superconductivity in that it does not depend solely on the high-energy electron-boson interaction to account for the high T_c. Rather, it is the cooperative nature of both the electron-phonon interaction and the electronic electron-boson interaction which results in significantly increased critical temperatures.
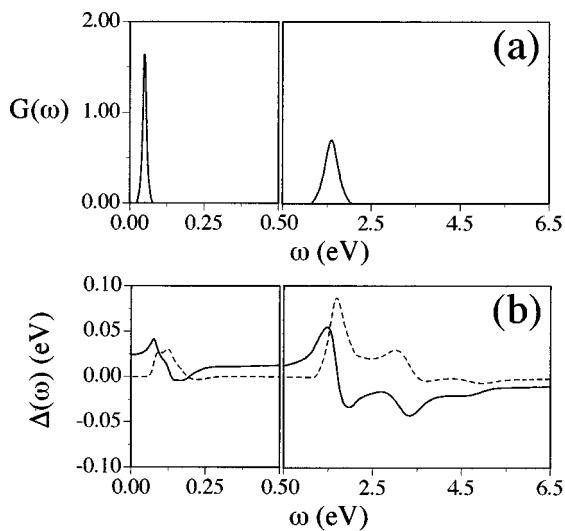

FIG. 14. The joint HTS electron-boson-based pairing mechanism. (a) A model $G(\Omega)$ consisting of an electron-phonon interaction *and* an electronic electron-boson interaction centered at 1.6 eV. (b) The zero-temperature $\Delta(\omega)$ obtained using the $G(\Omega)$ in (a). The parameters and results of these calculations are shown in joint HTS coupling section of Table II.

V. SUMMARY

In this paper we have described the numerical integration techniques used to solve the finite-temperature real-energy-axis Eliashberg equations. This algorithm was developed as a means of obtaining a high precision $\Delta(\omega,T)$ based upon an arbitrary form of the electron-boson coupling function and the magnitude of the effective Coulomb repulsion. We have presented a number of solutions of the Eliashberg equations which illustrate the manner in which different input parameters, such as $G(\Omega)$, μ^*, and T, affect the functional form of $\Delta(\omega,T)$.

The Eliashberg formalism provides an important link between experiment and theory, provided the correct input to the theory is known. The results of experiments which cannot be accounted for within the BCS formalism may often be accounted for within the full Eliashberg description of the superconducting state. The algorithm described in this paper was developed to aid in the interpretation of these experiments.

The primary use of this algorithm in our group has been in the interpretation of optical experiments performed on the high-temperature cuprate superconductors. With these experimental data, and the results of the finite-temperature Eliashberg calculations, we proposed the existence of a joint electron-boson coupling mechanism. By assuming that the operative electron-boson coupling function consisted of both an electron-phonon component and a high-energy electron-boson interaction, we were able to solve for both the temperature and energy dependence of the structure observed in the high precision superconducting-to normal-state reflectance ratio of these materials.[10] Based upon our model $G(\Omega)$, the observed structure in the optical spectra and the high T_c are natural consequences of the theory, thus demonstrating the importance of the finite-temperature Eliashberg description of the superconducting state in experiments which cannot be accounted for in the usual BCS description.

[1] G. M. Eliashberg, Sov. Phys. JETP **11**, 696 (1960).

[2] J. Bardeen, L. N. Cooper, and J. R. Schrieffer, Phys. Rev. **108**, 1175 (1957).

[3] P. B. Allen and B. Mitrovic, in *Solid State Physics: Advances in Research and Applications*, edited by H. Ehrenreich, F. Seitz, and D. Turnbull (Academic, New York, 1982), Vol. 37, p. 1.

[4] D. J. Scalapino, in *Superconductivity*, edited by R. D. Parks (Dekker, New York, 1969), Vol. 1, p. 449.

[5] W. L. McMillan and J. M. Rowell, in *Superconductivity* (Ref. 4), p. 561.

[6] R. Merservey and B. B. Schwartz, in *Superconductivity* (Ref. 4), p. 117.

[7] D. M. Ginsberg and L. C. Hebel, in *Superconductivity* (Ref. 4), p. 193.

[8] V. Z. Kresin and S. A. Wolf, *Fundamentals of Superconductivity* (Plenum, New York, 1990).

[9] M. J. Holcomb, J. P. Collman, and W. A. Little, Phys. Rev. Lett. **73**, 2360 (1994).

[10] M. J. Holcomb *et al.*, Phys. Rev. B **53**, 6734 (1996).

[11] G. Bergmann and D. Rainer, Z. Phys. A **263**, 59 (1973).

[12] G. D. Mahan, *Many-Particle Physics* (Plenum, New York, 1981).

[13] P. B. Allen and R. C. Dynes, Phys. Rev. B **12**, 905 (1975).

[14] J. P. Carbotte, Rev. Mod. Phys. **62**, 1027 (1990).

[15] D. J. Scalapino, J. R. Schrieffer, and J. W. Wilkins, Phys. Rev. **148**, 263 (1966).

[16] H. J. Vidberg and J. W. Serene, J. Low Temp. Phys. **29**, 179 (1977).

[17] F. Marsiglio, M. Schossmann, and J. P. Carbotte, Phys. Rev. B **37**, 4965 (1988).

[18] P. Morel and P. W. Anderson, Phys. Rev. **125**, 1263 (1962).

[19] D. J. Scalapino, Y. Wada, and J. C. Swihart, Phys. Rev. Lett. **14**, 102 (1965).

[20] W. L. McMillan, Phys. Rev. **167**, 331 (1968).

[21] N. Miyakawa *et al.*, J. Phys. Soc. Jpn. **62**, 2445 (1993).

[22] S. D. Brorson *et al.*, Solid State Commun. **74**, 1305 (1990).

[23] G. L. Eesley *et al.*, Phys. Rev. Lett. **65**, 3445 (1990).

[24] GAPCALC 1.0, written by M. J. Holcomb, copyright © 1995 The Board of Trustees of the Leland Stanford Junior University, Stanford, CA. All Rights Reserved.

[25] The upper-energy cutoff limit of this integration extends to approximately five times the limit used in Eq. (1). This assures the proper high-energy behavior of $Z(\omega,T)$.

[26] N. N. Bogoliubov *et al.*, *A New Method in the Theory of Superconductivity (1958)* (Consultants Bureau, New York, 1959).

[27] E. L. Wolf and G. B. Arnold, Phys. Rep. **91**, 31 (1982).

[28] A. A. Galkin *et al.*, Sov. Phys. JETP **39**, 1115 (1974).

[29] R. Akis and J. P. Carbotte, Solid State Commun. **78**, 393 (1991).

[30] P. B. Allen and D. Rainer, Nature (London) **349**, 396 (1991).

[31] P. Vashishta and J. P. Carbotte, Phys. Rev. B **7**, 1874 (1972).

[32] J. Blezius *et al.*, Phys. Rev. B **38**, 179 (1988).

[33] R. Akis and J. P. Carbotte, Physica C **157**, 395 (1989).

[34] V. Z. Kresin and V. P. Parkhomenko, Sov. Phys. Solid State **16**, 2180 (1975).

[35] L. C. Hebel and C. P. Slichter, Phys. Rev. **107**, 901 (1957).

[36] L. C. Hebel and C. P. Slichter, Phys. Rev. **113**, 1504 (1959).

[37] A. E. Karakozov, E. G. Maksimov, and A. A. Mikhailovsky, Solid State Commun. **79**, 329 (1991).

[38] We use the approximate formula, $\Delta_0(T) = \Delta_0(0)\{1 - (T/T_c)^{3.52}\}^{0.55}$, to describe the temperature dependence of the BCS gap.

[39] The functional forms of the $G(\Omega)$ used in these calculations include models possessing one Lorentzian peak, and models consisting of two Lorentzian peaks with one peak at energy ω_0, and the other peak at either $2\omega_0$, $4\omega_0$, or $8\omega_0$.

[40] B. Mitrovic *et al.*, Phys. Rev. B **29**, 6187 (1984).

[41] H. Rietschel *et al.*, Phys. Rev. B **22**, 4284 (1980).

[42] G. Chen *et al.*, Phys. Rev. B **48**, 13 959 (1993).

[43] I. I. Mazin *et al.*, Phys. Rev. B **47**, 538 (1993).

[44] G. Bergmann and D. Rainer, Z. Phys. A **263**, 59 (1973).

[45] V. Z. Kresin, H. Gutfreund, and W. A. Little, Solid State Commun. **51**, 339 (1984).

[46] S. B. Nam, Phys. Rev. **156**, 470 (1967).

[47] W. Shaw and J. C. Swihart, Phys. Rev. Lett. **20**, 1000 (1968).

[48] W. A. Little, in *Novel Superconductivity*, edited by S. A. Wolf and V. Z. Kresin (Plenum, New York, 1987).

[49] V. Z. Kresin and H. Morawitz, Phys. Rev. B **37**, 7854 (1988).

[50] W. A. Little, Phys. Rev. **156**, 396 (1964).

[51] V. L. Ginzburg, Sov. Phys. Usp. **13**, 335 (1970).

[52] D. Allender, J. Bray, and J. Bardeen, Phys. Rev. B **7**, 1020 (1972).

[53] H. Guffreund and W. A. Little, in *Highly Conducting One Dimensional Solids*, edited by J. T. Devreese, R. P. Evard, and V. E. Doren (Plenum, New York, 1979), p. 305.

[54] This is in agreement with the approximate results obtained by Kresin and Morawitz (Ref. 49) in the context of a joint electron-phonon electron-plasmon model of high-T_c superconductivity.